2006

A Thermodynamic Property Chart as a Visual Aid to Illustrate the Interference Between Expansion Work Recovery and Internal Heat Exchange

Stefan Elbel
University of Illinois at Urbana-Champaign

Predrag Hrnjak
University of Illinois at Urbana-Champaign

A THERMODYNAMIC PROPERTY CHART AS A VISUAL AID TO ILLUSTRATE THE INTERFERENCE BETWEEN EXPANSION WORK RECOVERY AND INTERNAL HEAT EXCHANGE

Stefan ELBEL, Predrag HRNJAK[a]

Department of Mechanical and Industrial Engineering
University of Illinois at Urbana-Champaign
1206 West Green Street, Urbana, IL 61801, USA
[a](Phone: +1-217-244 6377, Fax: +1-217-333 1942, Email: pega@uiuc.edu)

ABSTRACT

Expansion work recovering devices (EWRDs) such as the refrigerant ejector or expander can significantly improve the cycle efficiency of transcritical R744 systems by approaching isentropic expansion. This paper uses a thermodynamic property chart to visualize the work recovery potentials of such devices. Two distinguished cases regarding the operational characteristics of an internal heat exchanger (IHX) are discussed and the possible interferences with the EWRD potentials are analyzed. The thermodynamic property chart reveals how the use of an IHX reduces the EWRD potential by competing for the same temperature difference. While the assessments of the effects on cooling capacity are readily available, it is generally more complex to predict the associated changes in COP. Thus, a numerical system model is used to address the issue of how efficient the EWRD has to be in order to reduce or eliminate the need for an IHX. For the system investigated it was found than an approximately 50% efficient ejector can replace a 60% effective IHX in order to achieve identical COPs at a given cooling capacity in a transcritical R744 cycle.

1. INTRODUCTION

Throttling losses associated with isenthalpic expansion in transcritical R744 systems are known to be responsible for a significant reduction of the overall cycle efficiency. The losses generally become more pronounced as the pressure difference across the expansion device increases, resulting in larger deviations between lines of constant specific entropy and specific enthalpy in appropriate thermodynamic charts. This paper investigates the theoretical potentials of expansion work recovering devices, such as the refrigerant expander or ejector. The common characteristic of these devices is that they attempt to approach isentropic expansion rather than isenthalpic throttling of the working fluid. In case both devices could be operated without any losses, the recoverable amounts of expansion work would be identical for the expander and the ejector. Of particular interest is the interaction of the expansion work recovering device with the internal heat exchanger which is commonly found in the transcritical R744 cycle. Even though the primary function of an internal heat exchanger is to increase the cooling capacity of a given cycle which is accomplished by a simultaneous increase in compressor work (which, depending on the fluid properties, may or may not proportionally increase more than the gain in capacity, resulting in a negative, neutral or even positive effect on system COP), the use of the additional heat exchanger interferes with the potential of recoverable expansion work. The interference arises, because the internal heat exchanger minimizes throttling losses by shifting the expansion process into property regions where lines of constant specific enthalpy follow the lines of constant specific entropy more closely. The thermodynamic temperature-specific entropy chart (Ts) can be used to visualize the interference between isentropic expansion process and internal heat exchange. Energy transfer processes by heat and work within the cycle of interest can be interpreted in terms of areas in the according Ts-diagram. In addition, the expansion work recovery potential can be illustrated by an area representation as well. The mechanism of internal heat exchange is included in the same diagram, revealing the competition for the same temperature difference as the isentropic expansion device. For the internal heat exchanger, two general cases are discussed which distinguish themselves depending on at which side of the component the minimum heat capacity rate is located. Furthermore, numerical results obtained from a comprehensive system model are used to answer the question of how efficient the expansion work recovery device has to be in order to reduce or eliminate the need for internal heat exchange.

2. REPRESENTATION OF THE THROTTLING LOSSES IN THE Ts-DIAGRAM

A typical Ts-diagram for a standard R744 vapor compression cycle without IHX is shown in Figure 1. The air-conditioning cycle is operated in transcritical mode and based on the following idealized assumptions: isobaric heat rejection at 11MPa in the gas cooler with an approaching temperature difference of 0^oC, isenthalpic expansion (throttling) in the expansion valve, isobaric heat addition at 4MPa in the evaporator, and isentropic compression in the single-stage compressor starting from the saturated vapor line.

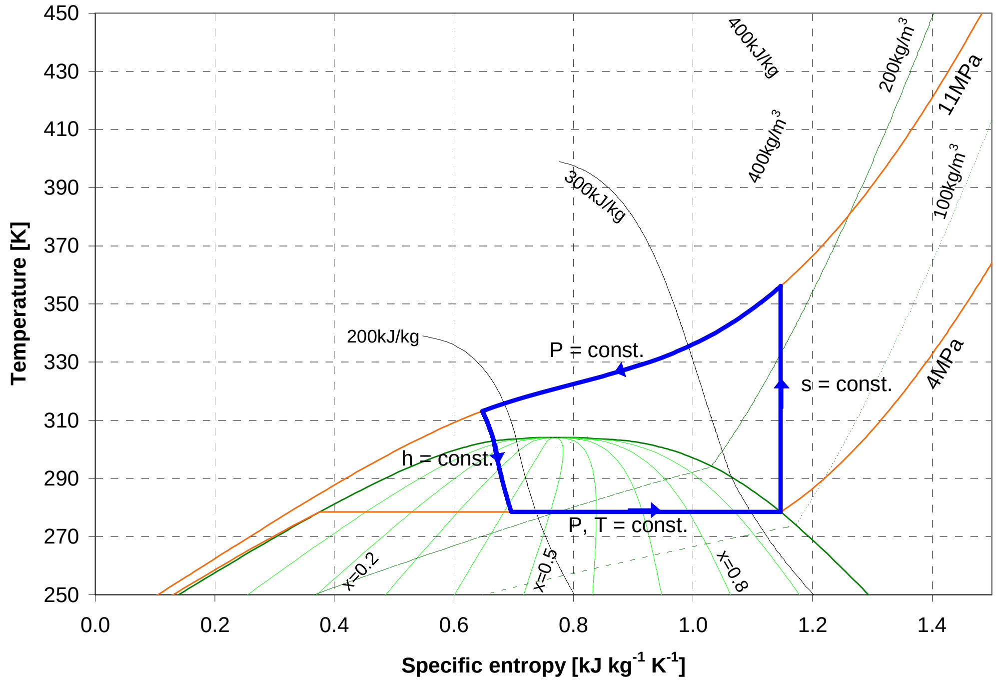

Figure 1: Ts-diagram showing a transcritical R744 air-conditioning cycle without internal heat exchange

Equation (1) demonstrates that in a Ts-diagram, the area underneath the curve connecting two different refrigerant states can be interpreted as a graphical representation of the heat transferred by the connecting process.

$$q = \int_{1\to 2} \delta q = \int_{1}^{2} T ds \qquad (1)$$

Thus, the (larger) heat rejection area is obtained by applying equation (1) between the inlet and the outlet states of the gas cooler. Similarly, the (smaller) heat addition area is obtained from the inlet and outlet states of the evaporator. Because both the compressor and the expansion valve are assumed to operate adiabatically and since conservation of energy prohibits any change in total energy in a closed steady-state cycle, the net work transferred to the cycle has to be equal to the difference between these two areas (net heat). In other words, in a Ts-diagram the net work transferred is represented by the area enclosed by the cycle. Of particular interest is the amount of work lost during the throttling process which is shown in an enlarged portion of the Ts-diagram in Figure 2 with the ordinate not being drawn to scale. The isenthalpic expansion from 1→2 increases the net work of the cycle by the size of the hatched area $A_{2\text{-a-b-3-2}}$ in comparison to a cycle having isentropic expansion from 1→3. By using equation (1) and the fundamental Tds relation shown in equation (2) it can be proved that this area equals area $A_{1\text{-3-4-5-c-d-6-7-1}}$ outlined in Figure 2.

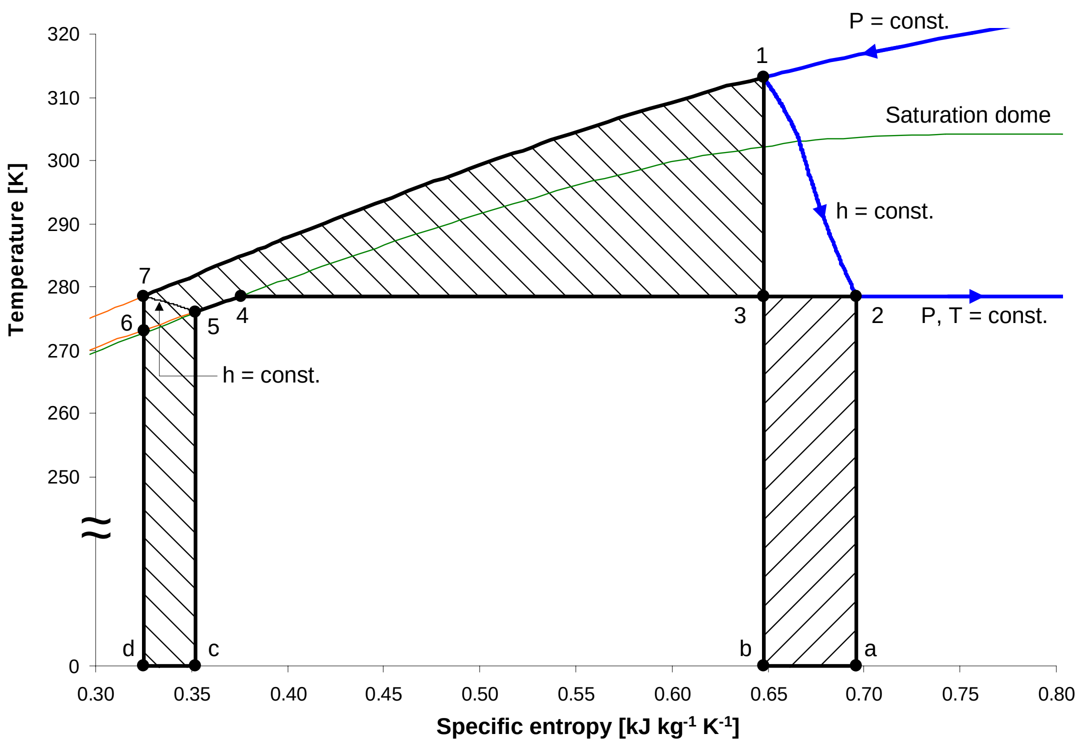

Figure 2: Throttling losses of a transcritical R744 system visualized in a Ts-diagram

$$Tds = dh - vdP \tag{2}$$

$$A_{2-a-b-3-2} = \int_{2\to 3} \delta q = \int_2^3 Tds = \int_2^3 [dh - vdP] = h_2 - h_3 \tag{3}$$

$$A_{3-b-c-5-4-3} = \int_{5\to 3} \delta q = \int_5^3 Tds = \int_5^3 [dh - vdP] = h_3 - h_5 \tag{4}$$

$$A_{1-3-4-5-c-d-6-7-1} + A_{3-b-c-5-4-3} = \int_{7\to 1} \delta q = \int_7^1 Tds = \int_7^1 [dh - vdP] = h_1 - h_7 \tag{5}$$

In equations (3), (4), and (5) the vdP terms vanish, because each of the initial and final states are at identical pressures. Also, from Figure 2 it is apparent that h_1 equals h_2 and h_7 equals h_5, leading to equation (6).

$$A_{1-3-4-5-c-d-6-7-1} = h_2 - h_5 - A_{3-b-c-5-4-3} = h_2 - h_3 = A_{2-a-b-3-2} \tag{6}$$

Equation (7) can be proved with similar reasoning.

$$A_{4-5-c-d-6-7-4} = \int_4^7 vdP \tag{7}$$

Many thermodynamic texts such as Cerbe and Hoffman (1999) often render the vdP term in equation (7) negligible, which results in equation (8).

$$A_{2-a-b-3-2} \approx A_{1-3-4-7-1} \tag{8}$$

While equation (8) might be a suitable approximation for a subcritical cycle in combination with a fluid having a relatively small difference between the condensation and the evaporation pressure (e.g. R134a), the situation is quite different for transcritical R744 air-conditioning applications. Also, the liquid density of R744 is lower than that of R134a at identical evaporation temperature, further increasing the vdP term. In comparison to an R134a cycle operating at comparable ambient conditions as the R744 cycle described in Figure 1, the vdP term in equation (7) represents approximately 20% of the net work for R744, while it is only 3% for R134a. Thus, the throttling loss of an R744 cycle should be represented by its exact area outlined in the Ts-diagram (Figure 2) rather than by the approximation according to equation (8).

3. MECHANISM AND LIMITS OF THE IHX

Usually, an IHX is added to a standard vapor compression cycle (Figure 3) to increase its cooling capacity. The capacity gain comes at some cost, namely an increase in compressor power due to more superheated compressor inlet conditions. This compressor work increase can be seen in the pressure-specific enthalpy (Ph) diagram, where the new compression process follows a more horizontal isentrope. However, expansion losses are reduced if a high pressure fluid is expanded from colder temperatures, because the isentropes in the Ph-diagram become almost vertical lines in the region of subcooled liquid. Depending on the thermodynamic characteristics of the working fluid, the gain in capacity can grow faster than the increase in net work rate as demonstrated by Domanski *et al.* (1994) in equation (9).

$$COP_{with.IHX} \approx COP_{without.IHX}\left(1+\frac{\Delta\dot{Q}}{\dot{Q}}-\frac{\Delta\dot{W}}{\dot{W}}\right) \tag{9}$$

For these fluids, and R744 is among them, the use of an IHX increases the cycle COP as well. For transcritical R744 cycles in particular, the use of an IHX also reduces the pressure ratio of the compressor, because the IHX lowers the performance maximizing high-side pressure as discussed by Kim *et al.* (2003). Thus, the reduced compression ratio further increases the cycle COP.

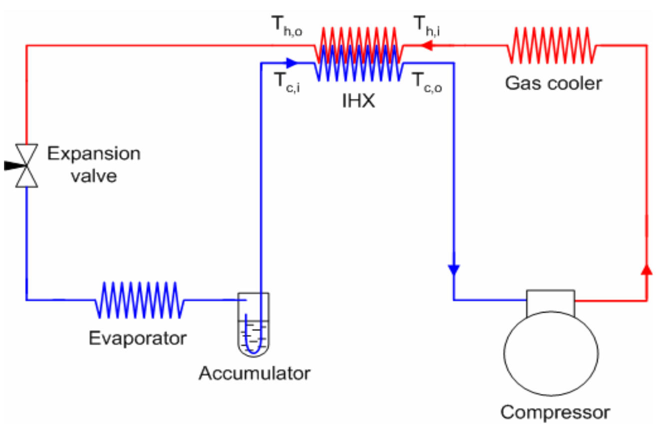

Figure 3: Typical system layout of a transcritical R744 system having an internal heat exchanger

Provided the IHX can be treated adiabatically with respect to its surroundings, its effectiveness for counterflow operation is defined by equations (10), (11a), and (11b).

$$\varepsilon=\frac{\dot{Q}}{\dot{Q}_{\max}}=\frac{\dot{Q}}{C_{\min}\cdot\Delta T_{\max}}=\frac{\dot{Q}}{(\dot{m}\cdot\bar{c}_p)_{\min}\cdot(T_{h,i}-T_{c,i})} \tag{10}$$

$$\dot{Q}=(\dot{m}\cdot\bar{c}_p)_{HPS}\cdot(T_{h,i}-T_{h,o}) \tag{11a}$$

$$\dot{Q}=(\dot{m}\cdot\bar{c}_p)_{LPS}\cdot(T_{c,o}-T_{c,i}) \tag{11b}$$

Depending on if the minimum heat capacity rate C_{min} is located on the high pressure side (HPS) or the low pressure side (LPS) of the IHX two different cases are possible as outlined in Figure 4.

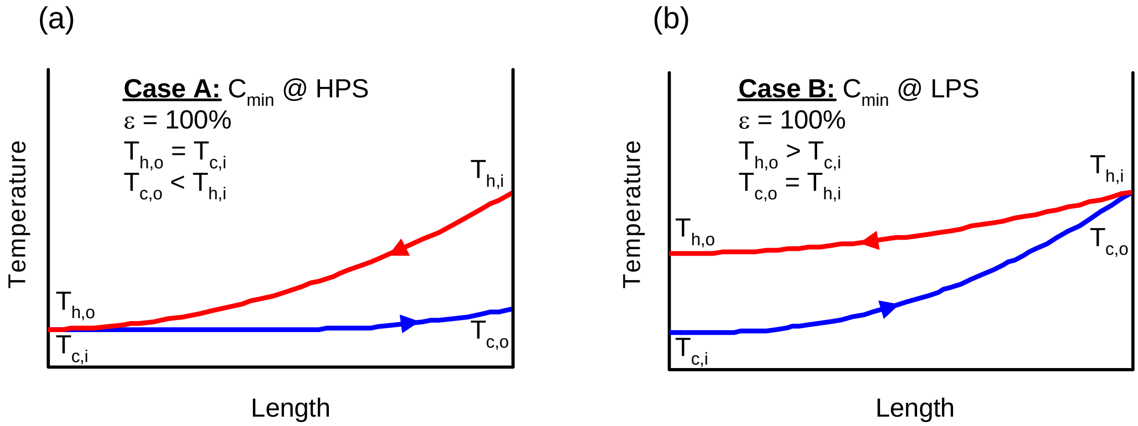

Figure 4: Possible IHX operation modes depending on the location of C_{min}

For both cases, ε = 100% was assumed which, theoretically, can be achieved by an infinitely long heat exchanger. In Figure 4a (Case A), where C_{min} is on the HPS, the refrigerant temperature at the inlet to the expansion valve is cooled down to the temperature of the refrigerant at the evaporator exit. In a real IHX, the difference between these two temperatures determines its effectiveness according to equations (10) and (11a). Even though there might be two-phase flow at the inlet of the IHX's LPS with an infinitely large specific heat, averaged values lower than infinity can be determined over the whole length of the IHX. Due to the difference in average specific heats on the HPS and the LPS, the compressor suction temperature is always lower than the refrigerant temperature at the gas cooler exit, even for a 100% effective IHX.

In contrary, if C_{min} is on the IHX's LPS (Case B, Figure 4b), the compressor suction temperature is heated until it reaches the refrigerant temperature at the gas cooler exit, or, in case of the earlier assumption that the approaching temperature difference equals $0^{o}C$, the ambient air temperature at the gas cooler inlet. For this case, the difference in average specific heats on the LPS and the HPS cause the temperature at the inlet to the expansion valve to be always higher than the saturated evaporation temperature, even for a 100% effective IHX. The effectiveness of a real IHX is calculated with equations (10) and (11b) in this case. The refrigerant exit quality at the evaporator dictates if the IHX is operated at Case A or B. For typical conditions encountered in many air-conditioning and heat pumping applications, the IHX has its minimum heat capacity rate on the low pressure side (Case B).

4. EXPANSION WORK RECOVERY AND INTERNAL HEAT EXCHANGE

Even though the illustration of the work recovery potential in a Ts-diagram is more readily available for the refrigerant expander, it can principally be constructed for an ejector system in a similar fashion. However, the area representation in a chart with underlying intensive property axes gets more complicated as the refrigerant mass flow rates through the heat rejection side (gas cooler) typically differs from that of the heat absorption side (evaporator) by the nature of the ejector system. Thus, Lorentzen (1983) suggested the use of a Tms- = TS-diagram instead. Nevertheless, the following discussion is based on expander diagrams to facilitate general understanding.

If the pressure reduction from the HPS to the LPS takes place in an isentropic EWRD instead of in an expansion valve, the net work of the cycle decreases. The rate of shaft work extracted by the device is equal to the gain in cooling capacity as demonstrated in Figure 2. This is because isentropic expansion results in lower specific enthalpies at the evaporator inlet. Figure 5 presents two different cycles in a Ts-diagram employing expansion valves. The cycle enclosing the smaller area (square markers) is the baseline without IHX while the other one (round markers) shows an expansion valve cycle having a perfect IHX, representing Case B in Figure 4.

In case an EWRD is used but no IHX, the gain in cooling capacity is proportional to area A6. The use of an IHX in combination with an expansion valve increases the cooling capacity by an amount proportional to A5 + A6, showing that the IHX can provide more additional cooling capacity than the EWRD, provided the compressor mass flow remains constant. The capacity transferred by the IHX is equal to the gain in cooling capacity and proportional to A7. At the same time it can be seen how the use of an IHX is responsible for letting the work recovery potential shrink, as demonstrated by the difference between areas A6 and A4, respectively. More work can be recovered for larger temperature differences across the expansion device ($\Delta T1 > \Delta T2$, thus A6 > A4), showing that the EWRD and the IHX are actually competing for the same temperature difference. It can be deducted from Figure 5 that an IHX having its C_{min} on the HPS (Case A in Figure 4) would further reduce the available temperature difference, which, for a 100% effective IHX would totally annihilate the potential for recovering any of the throttling losses. However, this scenario can theoretically only occur for very low refrigerant qualities at the exit of the evaporator, caused by shifting C_{min} from the LPS to the HPS of the system.

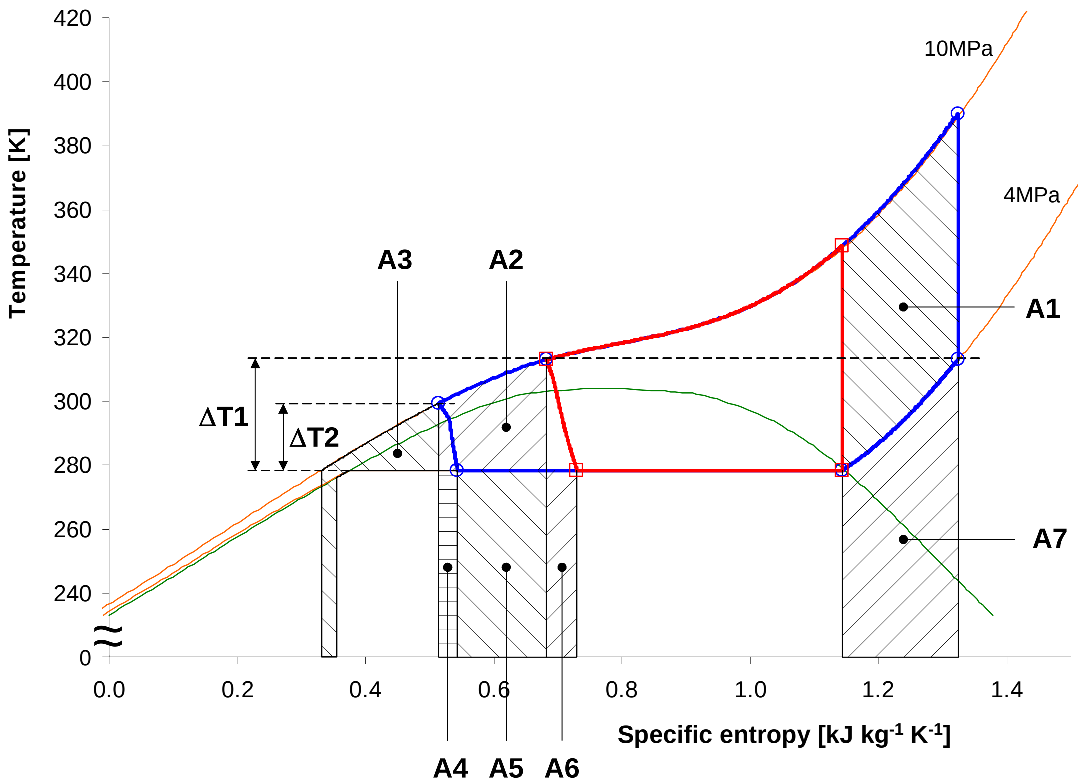

Figure 5: Influence of IHX on expansion work recovery potential

While it is more apparent how both IHX and EWRD influence the cooling capacity, it is generally more difficult to assess the effects on COP. The IHX in the expansion valve cycle increases the net work by A1, whereas the EWRD reduces the net power by A2 + A3 of the cycle without IHX. At the same time it can be seen that the EWRD in combination with an IHX reduces the net power by only A4. However, in real systems some of the EWRD's COP improvement can be traded for additional cooling capacity. Thus, the question of how efficient the EWRD has to be in order to replace the IHX still needs to be answered. To address this issue, a comprehensive system model for mobile air-conditioning applications was used. This was done, because the foregoing analysis of the thermodynamic cycles did not take into account any realistic system effects, such as finite heat exchanger areas, pressure drops on both air and refrigerant sides, or the change of compressor mass flow rate as a function of the suction condition, just to name a few. The model is based of a set of approximately 2,500 generally non-linear time-independent equations solved simultaneously with EES (F-Chart Software, 2005). While Robinson and Groll (1998) numerically analyzed cycles with internal heat exchange and expansion turbines, the EWRD investigated here is a refrigerant ejector. The model is capable of simulating expansion valve as well as ejector cycles both with and without having an IHX. The features of the R744 ejector as well as more detailed information regarding the simulation model are given by Elbel and Hrnjak (2004). Simulation results are presented in Figure 6. The test condition investigated had a temperature of 35°C (indoor and outdoor); the relative humidity of the air entering the evaporator was 40%. The indoor air flow and outdoor air flow rates were 425m^3/hr and 3058m^3/hr, respectively. The speed of the 33cm^3 open-shaft compressor was adjusted such that the cooling capacity equaled 7.5kW in all simulation runs. Thus, the COPs of the different systems become directly comparable.

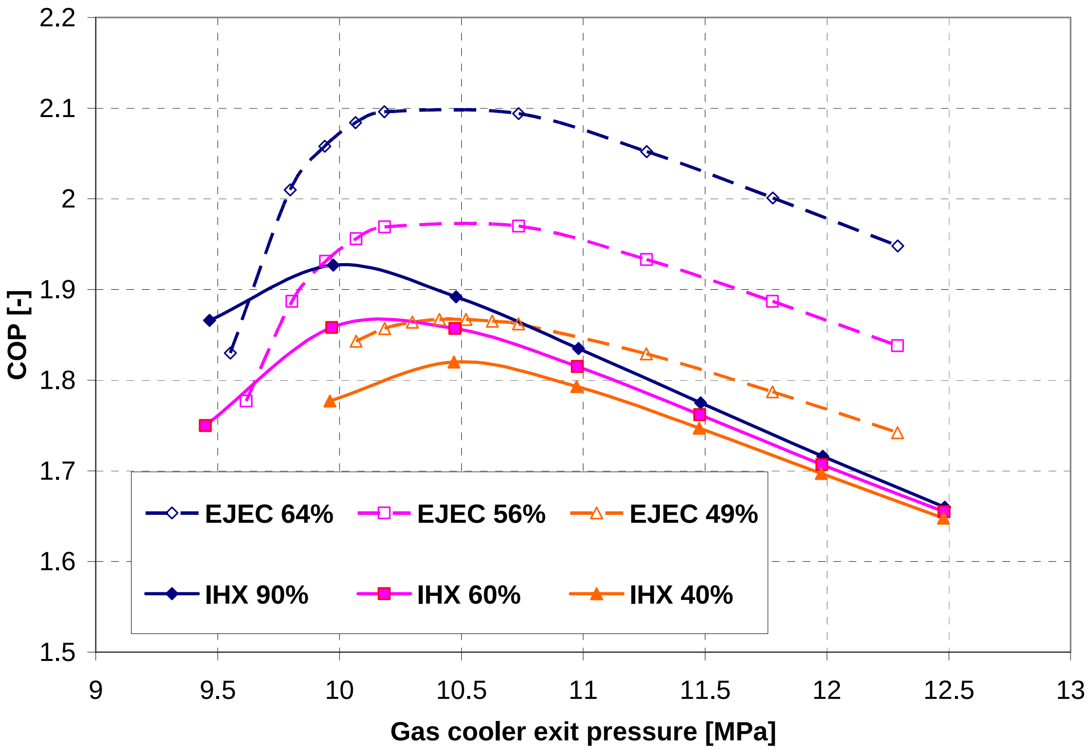

Figure 6: Required ejector efficiency to replace IHX for fixed cooling capacity (simulation results)

Figure 6 shows that the high-side pressure of a transcritical R744 system can be used to maximize the COP, regardless of the type of expansion device used. The solid curves represent results obtained for the system with expansion valve and different IHX effectiveness, whereas the dashed curves were calculated for a system without IHX having an ejector. The different ejector efficiencies shown were obtained by multiplying its individual component efficiencies and are to be understood as a measure of the overall deviation from isentropic expansion. As expected, for a more effective IHX the maximum COP increases and it occurs at a lower high-side pressure. A similar behavior can be observed for increasing ejector efficiencies. Furthermore, the line crossings reveal the ejector efficiency required to replace an IHX with a given effectiveness in an expansion valve system. For example at the test condition considered, a system having a 49% efficient ejector, but no IHX has approximately the same COP as an expansion valve system with a 60% effective IHX. Experimental results which confirm the numerical trends of a reduced need for internal heat exchange in transcritical R744 ejector systems are given by Elbel and Hrnjak (2006).

5. CONCLUSIONS

It was shown how a thermodynamic property chart can be used to visualize throttling losses which occur during isenthalpic expansion processes. In addition, the diagram reveals that throttling losses are more significant in transcritical R744 cycles than for conventional hydrofluorocarbons (HFC) / hydrochlorofluorocarbons (HCFC) refrigerants. The mechanism and limits of the internal heat exchange were discussed. At representative air-conditioning and heat pumping conditions, the minimum heat capacity rate is typically located on the low pressure side of the system. The interference between IHX and EWRD was discussed for this case and it was shown how the IHX reduces the potential of expansion work recovery by competing for the same temperature difference. A numerical system model revealed that theoretically, a 60% effective IHX can be eliminated from an expansion valve system when a 50% efficient ejector is used as the expansion device of a transcritical R744 system.

NOMENCLATURE

A	area	(kJ/kg)
C	heat capacity rate	(kW/K)
COP	coefficient of performance	(-)
$\bar{c}_p$	average specific heat	(kJ/kg-K)
EJEC	ejector	
EWRD	expansion work recovering device	
h	specific enthalpy	(kJ/kg)
HPS	high pressure side	
IHX	internal heat exchanger	
LPS	low pressure side	
$\dot{m}$	mass flow rate	(kg/s)
P	pressure	(kPa)
q	heat	(kJ/kg)
$\dot{Q}$	heat transfer rate	(kW)
S	entropy	(kJ/K)
s	specific entropy	(kJ/kg-K)
T	temperature	(K)
v	specific volume	(m^3/kg)
$\dot{W}$	power	(kW)
x	vapor quality	(-)

Subscripts

c	cold
h	hot
i	in
max	maximum
min	minimum
o	out

Greek

ε	effectiveness
Δ	difference

REFERENCES

Cerbe, G., Hoffmann, H.-J., 1999, *Einführung in die Thermodynamik*, Carl Hanser Verlag, München, 468 p.

Domanski, P.A., Didion, D.A., Doyle, J.P., 1994, Evaluation of suction-line/liquid-line heat exchange in the refrigeration cycle, *Int. J. Refrig.*, 17(7): 487-493

Kim, M.-H., Pettersen, J., Bullard, C.W., 2003, Fundamental process and system design issues in CO_2 vapor compression systems, *Prog. Energ. Combust.*, 30(2): 119-174

Lorentzen G., 1983, Throttling – the Internal Haemorrhage of the Refrigeration Process, *Proc. Inst. Refrig.*, Vol. 80: 39-47

Engineering Equation Solver - Academic Professional Version V7.457-3D, 2005, F-Chart Software, Middleton, WI

Robinson, D.M., Groll, E.A., 1998, Efficiencies of transcritical CO_2 cycles with and without an expansion turbine, *Int. J. Refrig.*, 21(7): 577-589

Elbel S.W., Hrnjak, P.S., 2004, Effect of Internal Heat Exchanger on Performance of Transcritical CO_2 Systems with Ejector, *Proc. 2004 Int. Refrig. Conf. Purdue*, Paper R166

Elbel, S., Hrnjak, P., 2006, Experimental Validation and Design Study of a Transcritical CO_2 Prototype Ejector System, *Paper to be presented at: 7th IIR Gustav Lorentzen Conference on Natural Working Fluids*, Trondheim, Norway, Paper 149

ACKNOWLEDGEMENT

The authors thankfully acknowledge the support provided by the Modine Manufacturing Company, the U.S. Army RDECOM, the DaimlerChrysler AG, and the Air-Conditioning and Refrigeration Center (ACRC) at the University of Illinois at Urbana-Champaign.